Organic Geochemistry 124 (2018) 12–21

Contents lists available at ScienceDirect

Organic Geochemistry

journal homepage: www.elsevier.com/locate/orggeochem

Improved chromatography reveals multiple new bacteriohopanepolyol isomers in marine sediments

Stephanie Kusch [a,b,*], Sunita R. Shah Walter [a,c], Jordon D. Hemingway [a], Ann Pearson [a]

[a] Department of Earth and Planetary Sciences, Harvard University, 20 Oxford St., Cambridge, MA 02138, USA
[b] Institute of Geology and Mineralogy, University of Cologne, Zülpicher Str. 49b, 50674 Cologne, Germany
[c] School of Marine Science and Policy, University of Delaware, 700 Pilottown Road, Lewes, DE 19958, USA

ARTICLE INFO

Article history:
Received 4 May 2018
Received in revised form 6 July 2018
Accepted 17 July 2018
Available online 18 July 2018

Keywords:
Bacteriohopanepolyols (BHPs)
BHP isomers
HPLC

ABSTRACT

Bacteriohopanepolyols (BHPs) are characterized by a large structural diversity, although methodological constraints have limited investigations of the occurrence of isomers among composite BHPs in environmental samples. Here, we describe a novel chromatography method that uses three serial Phenomenex Kinetex C_{18} columns to successfully resolve new structural isomers of BHPs commonly observed in marine sediment samples. The investigated samples consistently contain a high diversity of BHP isomers, but their relative abundances differ significantly between samples. These differences in relative abundance have potential to reflect different environmental conditions such as depositional setting or redox conditions. The improved BHP resolution and baseline separation of the new method is promising for accurate quantification and future environmental proxy development and compound-specific isotope work.

1. Introduction

Bacteriohopanepolyols (BHPs) are pentacyclic triterpenoids mainly synthesized by bacteria. The diagenetic products of BHPs (hopanols, hopanoic acids, and hopanes) are detectable in sedimentary rocks over timescales of millions to billions of years, respectively, making them excellent tracers for bacterial organic matter within the carbon cycle over much of Earth's history (Ourisson and Albrecht, 1992; van Dongen et al., 2006; Talbot et al., 2016). While this potential inspires great interest in understanding the environmental and taxonomic origins of BHPs recovered from sediments and the rock record, these origins remain largely elusive, particularly in the marine environment where metagenomic data indicate that BHP-producing bacteria predominantly belong to taxa that are yet uncharacterized (Pearson and Rusch, 2008).

BHPs have shown potential to carry information about both organism identity and environmental conditions. For example, 35-aminobacteriohopane-31,32,33,34-tetrol (aminotetrol) and 35-aminobacteriohopane-30,31,32,33,34-pentol (aminopentol) have so far been shown to be produced by aerobic methane oxidizing bacteria (Zundel and Rohmer, 1985; Talbot et al., 2003b; Coolen et al., 2008) and van Winden et al. (2012) suggested that isomers of aminotetrol could be indicative of acidophilic methanotrophs. However, isomers of both aminotetrol and aminopentol could not be detected in environmental moss or peat samples, most likely due to their low abundances. BHPs with highly functionalized side chains (composite BHPs) also seem to carry information about geographic and/or environmental conditions. Adenosyl-functionalized BHPs have proven valuable in detecting soil/riverine input into marine settings (Cooke et al., 2008; Zhu et al., 2011) while the ratio of two bacteriohopane-32,33,34,35-tetrol (BHT and BHT II) isomers has been suggested as proxy for water column suboxia or anoxia (Sáenz et al., 2011b), or even anaerobic ammonium-oxidation (anammox) in sedimentary records (Rush et al., 2014). However, complicating arguments for BHP source signatures, Eickhoff et al. (2014) observed increasing isomerization of BHT, 35-aminobacteriohopane-32,33,34-triol (aminotriol), and 32,35-anhydrobacteriohopanetetrol (anhydroBHT) during pressure- and temperature-based diagenetic experiments using biomass from *Rhodopseudomonas palustris* strain TIE-1 underscoring the need for better understanding of diagenetic effects. These examples suggest that the occurrence and abundance of composite BHP isomers may carry environmental information or information on organism biogeochemistry, but so far BHP isomer detection in environmental samples may have been hindered by low abundances (i.e., they may have been overlooked) and co-elution problems with established methods.

* Corresponding author.
E-mail addresses: stephanie.kusch@uni-koeln.de (S. Kusch), suni@udel.edu (S.R. Shah Walter), jordon_hemingway@fas.harvard.edu (J.D. Hemingway), apearson@eps.harvard.edu (A. Pearson).

https://doi.org/10.1016/j.orggeochem.2018.07.010
0146-6380/

Here, we describe a chromatographic method that resolves new structural BHP isomers and improves baseline separation of many BHPs. Significant differences in relative abundance of some of these isomers among various sedimentary settings highlight the need for good chromatographic separation to allow further development of BHP isomer-based proxies.

2. Materials and methods

2.1. Materials

Marine core-top sediments from the Santa Monica Basin (SMB-1 #1), the Gulf of Mexico (FCC-1), Cap Timiris (*GeoB*13609-4), the Benguela Upwelling (WW24005), and the Black Sea (P128, *GeoB*7606-2, *GeoB*7617-2/3, and *GeoB*7619-2) were analyzed (Fig. 1, Table 1). These samples represent various sedimentary settings including river-dominated to fully marine, open-ocean environments as well as oxic to anoxic redox conditions.

2.2. Methods

Samples were extracted using the modified Bligh and Dyer protocol of Sáenz et al. (2011a) with minor modifications. Samples were ultrasonicated twice in a mixture of methanol/dichlorome thane/water (2:1:0.8, v/v/v) for 1 h and then shaken for 3 h. A third ultrasonication step was performed in methanol/dichloromethane (1:1, v/v) for 30 min followed by final shaking for 1 h. Solvents were transferred into a separatory funnel, water/dichloromethane (1:1, v/v) was added, and the organic phase was liquid–liquid extracted from the aqueous phase using dichloromethane until it was colorless. In order to purify BHPs, the total lipid extract (TLE) was transesterified with 5% 6 N hydrochloric acid in methanol at 80 °C overnight and partitioned into hexane after addition of water. The transesterified TLE was then split into polarity fractions using hand-packed, pre-combusted (450 °C, 8 h) Flash silica gel columns employing a polarity elution pattern resolving 10 polarity fractions with BHPs eluting in 100% methanol (Pearson, 2000). The BHP-containing fraction was then acetylated using pyridine/acetic anhydride (50:50, v/v) at 50 °C for 1 h, re-dissolved in methanol/isopropanol (60:40, v/v), and filtered through 0.45 μm PTFE filters.

The effect of transesterification on artificial BHP synthesis (Schaeffer et al., 2008) was checked using an *R. palustris* TLE and no additional BHP structures or structural isomers could be detected (Fig. 2). However, we acknowledge that transesterification may have caused loss of sugar head groups of composite BHPs. We also observed a relative decrease in aminotriol, which might

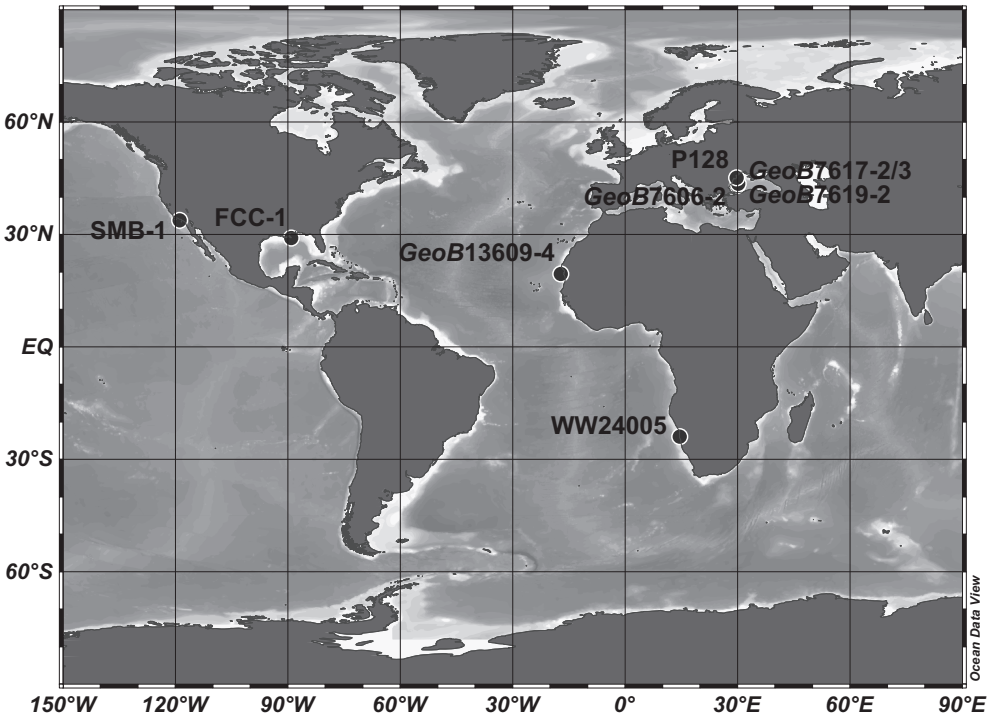

Fig. 1. Sample locations of core-top sediments used in this study.

Table 1
Core locations and sample information.

Sample	Cruise	Latitude [N]	Longitude [E]	Water depth [m]	Sediment interval [cm]	Sedimentary setting
P128	*R/V* Poseidon, P363	45.08528	29.78528	18	1–2	Oxic shelf, river-dominated
FCC-1	*R/V* Pelican	29.15708	−89.20154	27	1–4	Oxic shelf, river-dominated
WW24005	*R/V* A. von Humboldt, AHAB	−24.0000	−14.56916	85	13–15	Oxygen minimum zone, shelf, upwelling
*GeoB*13609-4	*R/V* M. S. Merian, MSM11/2	17.14278	−19.40917	918	0–1	Oxic, upper slope, upwelling
*GeoB*7617-2/3*	*R/V* Meteor, M51/4	43.63583	30.06694	464/467	fl, 0–1	Anoxic upper slope
*GeoB*7619-2	*R/V* Meteor, M51/4	43.48389	30.18556	1245	fl, 0–1	Anoxic intermediate slope
*GeoB*7606-2	*R/V* Meteor, M51/4	43.00250	29.98472	1809	fl, 0–1	Anoxic lower slope
SMB-1 #1	*R/V* Roger Revelle, Pulse-32	33.7333	−118.833	905	grab	Anoxic central basin

fl = fluffy layer.
* Samples from stations *GeoB*7617-2 and *GeoB*7617-3 were combined on board *R/V* Meteor during cruise M51/4 (Jorgensen et al., 2003).

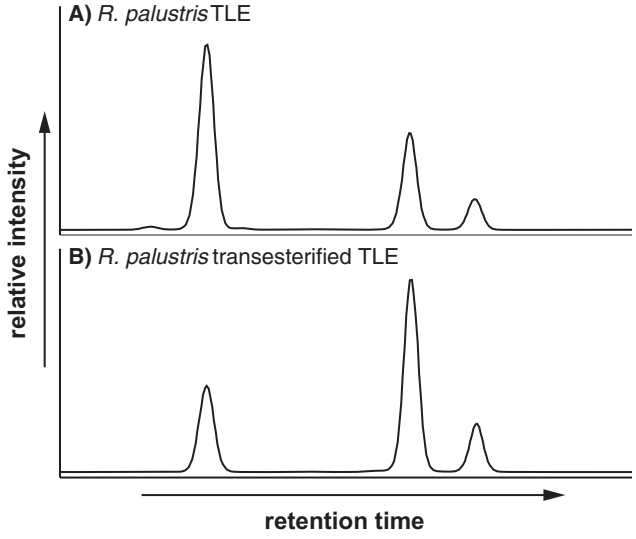

Fig. 2. MRM-based total ion chromatogram (TIC) of: (A) *R. palustris* TLE and (B) transesterified *R. palustris* TLE showing that no isomers of aminotriol, BHT, and 2Me-BHT were artificially produced during transesterification.

either be due to loss during transesterification or retention on the silica gel during column chromatography but may have also resulted from variable acetylation yields of independently processed *R. palustris* TLEs. In contrast, the results reported here were obtained from the same transesterified and acetylated sedimentary TLEs, so that any differences observed between chromatographic methods do not reflect wet chemical sample processing.

BHPs were separated using three Phenomenex Kinetex C_{18} columns (4.6 × 150 mm; 2.6 μm) in series maintained at 10 °C using an Agilent 1290 UHPLC system coupled to an Agilent 6410 QQQ mass spectrometer equipped with an atmospheric-pressure chemical ionization (APCI) source. Elution was achieved isocratically at 350 μl/min using a 60:40 (v/v) A/B mixture ratio from 0 to 80 min followed by back-flushing with both eluent C from 80 to 95 min and 60:40 (v/v) A/B from 95 to 115 min, and re-equilibration with 60:40 (v/v) A/B from 115 to 165 min (where A is 30:70 methanol/isopropanol, B is 90:10 methanol/water, and C is 90:10 ethyl acetate/methanol; v/v).

The APCI ion source settings were optimized for ionization efficiencies of BHT (*m/z* 655), aminotriol (*m/z* 714), 2β-methyl-bacteriohopane-32,33,34,35-tetrol (2βMe-BHT; *m/z* 669), and adenosylhopane (*m/z* 788) using the acetylated lipid extract of an *R. palustris* TIE-1 culture and were as follows: capillary voltage 3000 V, corona current 6 μA, vaporizer temperature 350 °C, gas temperature 325 °C, nebulizer 20 psig, and drying gas flow 4 ml/min. BHPs were identified in positive ion mode using multiple reaction monitoring (MRM) of transitions from the acetylated base peak precursor $[M+H]^+$ or $[MH–CH_3COOH]^+$ ions to the BHP-specific product ions *m/z* 191 and *m/z* 205 (A + B ring) with a fragmentor voltage of 100 V, a collision energy of 30 V, and a dwell time of 90 ms. BHPs were also analyzed following the gradient method of Talbot et al. (2003a) using one Phenomenex Kinetex C_{18} column (4.6 × 150 mm; 2.6 μm) and identical APCI and QQQ settings as above. For structural elucidation, the method was transferred to three Phenomenex Kinetex C_{18} columns (2.1 × 100 mm; 2.6 μm) in series (48.6 μl/min flow rate) and high-resolution mass spectra were generated using an Agilent 1200 nano HPLC system coupled to an Agilent 6520 Accurate-Mass Q-ToF mass spectrometer. APCI settings were identical and BHPs were identified via collision-induced dissociation (CID) in targeted MS^2 mode. The fragmentor voltage was 250 V, collision energy slope 3 V per 100 *m/z*, and acquisition rate 1 s/spectrum. The resolving power was 20,000 with an isolation width of 1.3 *m/z*, and mass accuracy of 100 ppm. Product ion mass spectra of the acetylated precursor ions were compared to previously published spectra (Talbot et al., 2007a, 2007b).

We report relative and semi-quantitative BHP abundances since reliable BHP quantification is hampered by the lack of commercially available authentic standards, and the large differences in ionization efficiency between surrogate standards such as 5α-pregnane-3β,20β-diol and BHPs with different moieties (van Winden et al., 2012; Wu et al., 2015) prevent accurate response factor determination. However, response factors should be identical between isomers of each BHP within a particular sample and across different samples allowing us to compare the BHP isomer distributions in the investigated samples.

3. Results and discussion

3.1. Identification of BHP structural isomers

The improved chromatography afforded by isocratic elution on three Kinetex C_{18} columns with an effective column length of 450 mm allows detection of several new structural isomers of BHPs commonly observed in marine sediments. Here, we describe isomers that were detected consistently above background in at least three different sediment samples with characteristic retention times (Fig. 3, Table 2) and for which high-resolution product ion spectra were obtained (Fig. 4). Five isomers of BHT (*m/z* 655; Fig. 4F–J) were detected including previously described BHT (*m/z* 655d) and BHT II (*m/z* 655e). A total of two isomers of anhydroBHT (*m/z* 613; Fig. 4M and N), unsaturated Δ^{11}-bacteriohopane-32,33,34,35-tetrol (unsat. BHT; *m/z* 653; Fig. 4K and L), and aminotriol (*m/z* 714; Fig. 4A and B) were identified. Additionally, three isomers of Me-BHT (*m/z* 669; Fig. 4C–E) were consistently detected. The corresponding high-resolution mass spectra show characteristic fragment ions, although some fragment ions have higher relative abundance at ±1 Da or ±2 Da (e.g., Fig. 4A and G), likely indicating either different isotope distributions or loss of H radicals. Overall, the concentration of most of these BHP isomers is very low in all samples and the background noise is high in some of the mass spectra, specifically *m/z* 653a (Fig. 4K) and *m/z* 613a (Fig. 4M). Since several characteristic fragment ions could be detected (see Fig. 4), we tentatively assign them as isomers of unsat. anhydroBHT and unsat. BHT, but acknowledge that additional work including higher mass accuracy is required to confirm our initial results. This will also aid in identifying further isomers; in addition to abovementioned isomers, we found several tentatively identified isomers including two isomers of unsaturated 32,35-anhydro-Δ^{11}-bacteriohopanetetrol, but concentrations were too low to obtain high-resolution mass spectra.

The stereochemistry of the new isomers remains unknown since both purity and quantity of isolated BHPs from marine sediments are too low to allow structural elucidation by ^{13}C NMR. Generally, the pentacyclic hopane skeleton of BHPs in bacterial cell membranes occurs in the "biological" 17β,21β configuration, which thermally epimerizes into the more stable "geological" 17α,21β configuration during diagenesis (Ourisson and Albrecht, 1992). The 17β,21β and 17α,21β configurations cannot be distinguished based on APCI product ion spectra unlike GC-based electrospray ionization (EI) mass spectra, which show characteristic differences in the abundance of the diagnostic *m/z* 191 and *m/z* 493 ions between these isomers (Talbot et al., 2008a). However, based on samples from a Holocene Antarctic lake sediment, Talbot et al. (2008a) report that 17α,21β-BHT elutes just prior to 17β,21β-BHT. Structural clues may, thus, be obtained from relative LC retention times, which should be comparable to the elution order of the

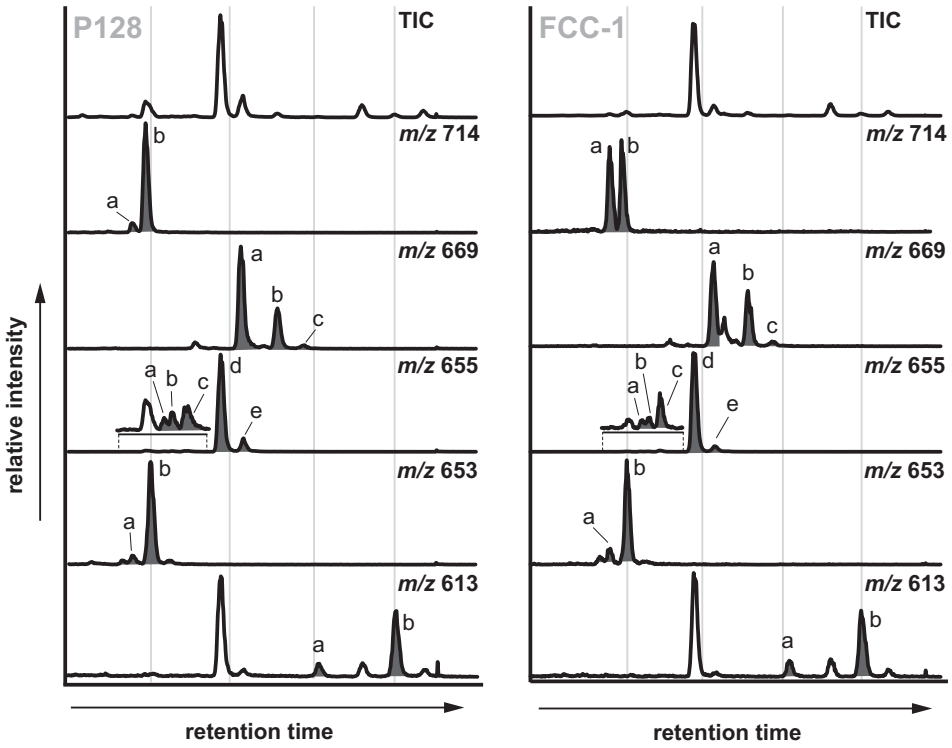

Fig. 3. MRM-based total ion chromatogram (TIC) and extracted ion chromatograms (EIC) of samples P128 and FCC-1 showing the chromatographic separation of up to five BHP isomers (arbitrarily labeled 'a' through 'e' based on retention time). EICs are scaled to the largest peak in each chromatogram. Compounds: *m/z* 714 aminotriol; *m/z* 669 Me-BHT; *m/z* 655 BHT; *m/z* 653 unsat. BHT; *m/z* 613 anhydroBHT.

Table 2
Semi-quantitative BHP isomer concentrations normalized to total lipid extract (1/g TLE) and relative to isomer *m/z* 669c in *GeoB*7619-2 (fluff). Isomers are arbitrarily labeled 'a' through 'e' based on retention time (see Fig. 2).

	m/z 613		*m/z* 653		*m/z* 655					*m/z* 669			*m/z* 714	
Sample	a	b	a	b	a	b	c	d[1]	e[2]	a[3]	b[4]	c	a	b
P128	3.1	14.4	11.7	262.0	32.1	35.2	22.8	2707.6	498.8	323.5	120.9	12.5	54.0	540.2
FCC-1	21.5	79.3	53.4	1011.8	126.8	107.3	221.6	18582.0	1118.3	862.1	643.3	49.6	404.5	211.0
WW24005	8.7	29.8	n.d.	7.0	17.8	n.d.	30.0	910.7	289.0	n.d.	14.7	n.d.	8.0	18.1
*GeoB*13609-4	20.5	87.5	14.5	222.4	25.5	53.4	116.8	4770.8	792.5	25.2	60.6	7.5	106.3	109.0
*GeoB*7617-2/3 (fluff #1)	4.7	17.6	8.8	581.0	n.d.	39.4	53.8	4173.4	477.0	35.3	18.3	5.4	24.7	242.0
*GeoB*7617-2/3 (fluff #2)	9.6	29.6	4.4	318.0	n.d.	14.8	49.4	2812.0	289.0	24.3	18.9	2.8	9.6	55.8
*GeoB*7617-2/3 (0–1 cm)	7.1	21.3	1.8	125.1	n.d.	9.3	48.8	1226.8	237.7	9.5	10.0	4.7	5.4	84.8
*GeoB*7619-2 (fluff)	n.d.	2.2	2.0	204.3	17.8	5.5	6.4	1710.0	63.3	21.4	9.1	n.d.	n.d.	272.3
*GeoB*7619-2 (0–1 cm)	7.0	17.6	n.d.	54.7	n.d.	6.1	21.3	568.9	118.3	6.3	2.0	1.7	3.0	122.3
*GeoB*7606-2 (fluff)	5.8	27.3	3.0	272.0	32.3	12.7	22.7	2822.6	163.5	24.8	6.9	1.0	9.5	17.1
*GeoB*7606-2 (0–1 cm)	24.0	43.9	14.0	613.9	n.d.	81.3	79.1	7628.6	485.8	63.1	17.6	4.4	17.3	9.6
SMB-1 #1	2.6	25.8	3.9	100.5	n.d.	40.3	28.3	2541.8	677.7	5.4	20.3	n.d.	15.2	166.9

n.d. – not detected.
[1] BHT.
[2] BHT II.
[3] 2βMe-BHT.
[4] 3βMe-BHT.

single-column method (Talbot et al., 2003a) with similar stationary phase and solvent scheme.

NMR-based identifications of the BHP side-chain stereoconfiguration, which is mostly linked via R configuration at C-22, have previously been confirmed for a subset of the BHPs identified in the samples analyzed here. NMR results indicate that the most abundant BHT isomer (*m/z* 655d usually referred to as "BHT") has the 32R,33R,34S configuration; another BHT isomer has the 32R,33R,34R configuration; and aminotriol has the 32R,33R,34S configuration (Neunlist and Rohmer, 1988; Bisseret and Rohmer, 1989; Zhao et al., 1996; Rosa–Putra et al., 2001). Given the high relative abundance of *m/z* 655e (BHT II of Sáenz et al., 2011b) in comparison to isomers *m/z* 655a through *m/z* 655c (Fig. 4) in this study, as well as its high abundance in certain bacterial cultures (Rush et al., 2014), this isomer is the most likely candidate for BHT with the 22R,32R,33R,34R-17β,21β configuration (Zhao et al., 1996; Rosa–Putra et al., 2001). However, Blumenberg et al. (2010) report BHT (*m/z* 655d) and a second isomer (most likely *m/z* 655e due to its elution after BHT) from sediments underlying the Benguela upwelling area. Upon periodic acid treatment, these authors found two isomers of 17β,21β-bishomohopanol in R and S configuration at C-22, respectively, indicating that BHT II may

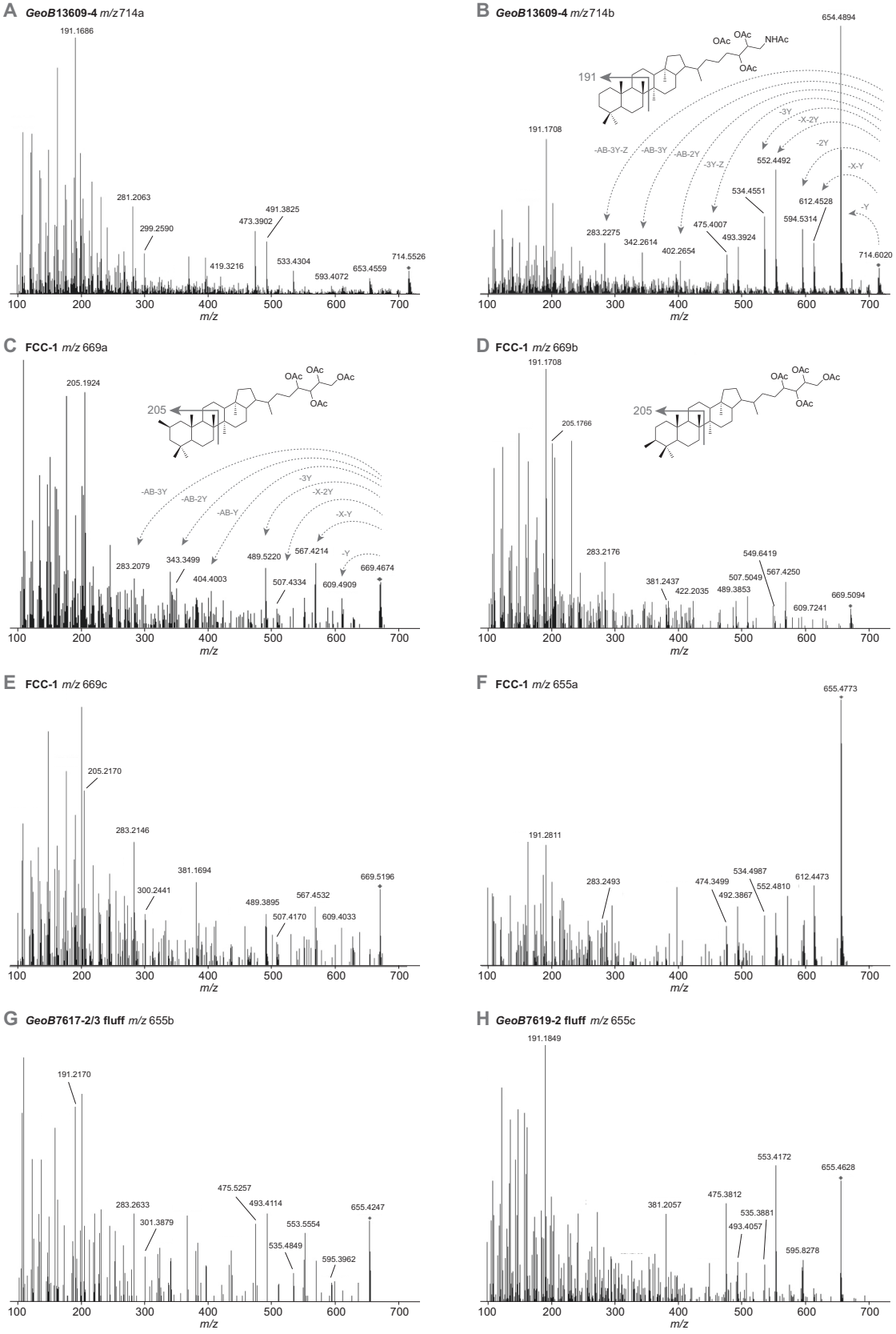

Fig. 4. High-resolution HPLC–APCI-Q-ToF mass spectra obtained in targeted MS^2 mode. Compounds: *m*/*z* 714 aminotriol; *m*/*z* 669 Me-BHT; *m*/*z* 655 BHT; *m*/*z* 653 unsat. BHT; *m*/*z* 613 anhydroBHT. Fragmentation is shown for major isomer of each compound: X = $COCH_3$, Y = CH_3COOH, Z = CH_3CONH_2, AB = A + B ring (C ring cleavage).

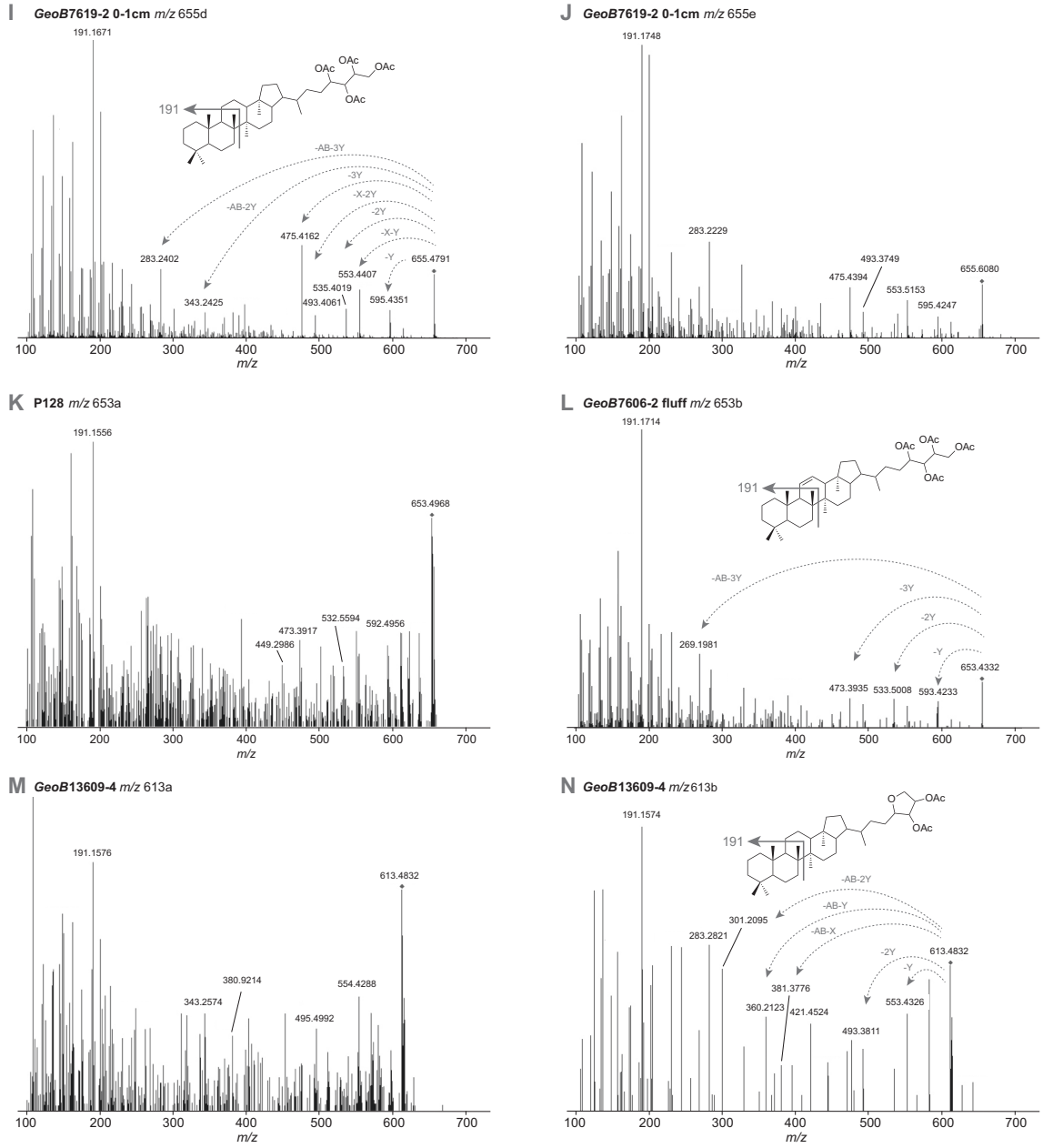

Fig. 4 (*continued*)

also have the 22S,32R,33R,34R or 22S,32R,33R,34S configuration (Blumenberg et al., 2010).

Based on the relative retention times in comparison to previously published chromatograms (Talbot et al., 2008b), the *m/z* 669a and *m/z* 669b Me-BHT isomers correspond to 2βMe-BHT and 3β-methyl-bacteriohopane-32,33,34,35-tetrol (3βMe-BHT), respectively. The low abundance isomer *m/z* 669c may either represent a different side chain configuration of 2βMe-BHT and/or 3βMe-BHT or a different stereoconfiguration at C-2. The latter possibility is supported by the occurrence of 2α-methyl-bacteriohopane-32,33,34,35-tetrol in a *Methylobacterium organophilum* culture extract (representing 5% of the 2Me-BHT epimers), despite the common belief that 2α-methylation is a thermal epimerization process (Stampf et al., 1991), which would preclude finding 2αMe-BHT in core-top sediments. Based on our data only, however, we cannot determine which stereoconfiguration is more likely.

Some BHP isomers observed here, including aminotriol and anhydroBHT, appear to be identical to those previously reported by Eickhoff et al. (2014) following treatment of *R. palustris* TIE-1 cell biomass at 170 °C. Based on relative retention times and relative abundances (Fig. 3), aminotriol isomers labeled *m/z* 714a (32R,33R,34S) and *m/z* 714b seem to correspond to the aminotriol isomers labeled *a* and *b* by Eickhoff et al. (2014), while anhydroBHT isomers labeled *m/z* 613a and *m/z* 613b seem to correspond to the anhydroBHT isomers labeled *b* and *c* by Eickhoff et al. (2014). In that study, GC–MS EI spectra obtained from the same samples revealed an even larger diversity of anhydroBHT isomers than that observed using LC–MS, all of which had 17β,21β configurations (Eickhoff et al., 2014). Despite the fact that these authors could not assign structural configurations of the respective BHP side chain moieties, such structural diversity provides promising opportunities to explore BHP distributions in response to environmental parameters.

3.2. Diversity and relative abundance of BHP isomers in marine sediments

The relative abundance of some BHP structural isomers varies strongly in the investigated sediment samples (Figs. 3 and 5). Overall, isomer abundances of most BHPs show one dominant isomer in most samples. Unsat. BHT and BHT are dominated by a major isomer, i.e., *m*/*z* 653b (94–100%; Fig. 5B) and *m*/*z* 655d (73–92%; Fig. 5C), respectively, and relatively regular patterns of minor isomers. In comparison, anhydroBHT shows significant

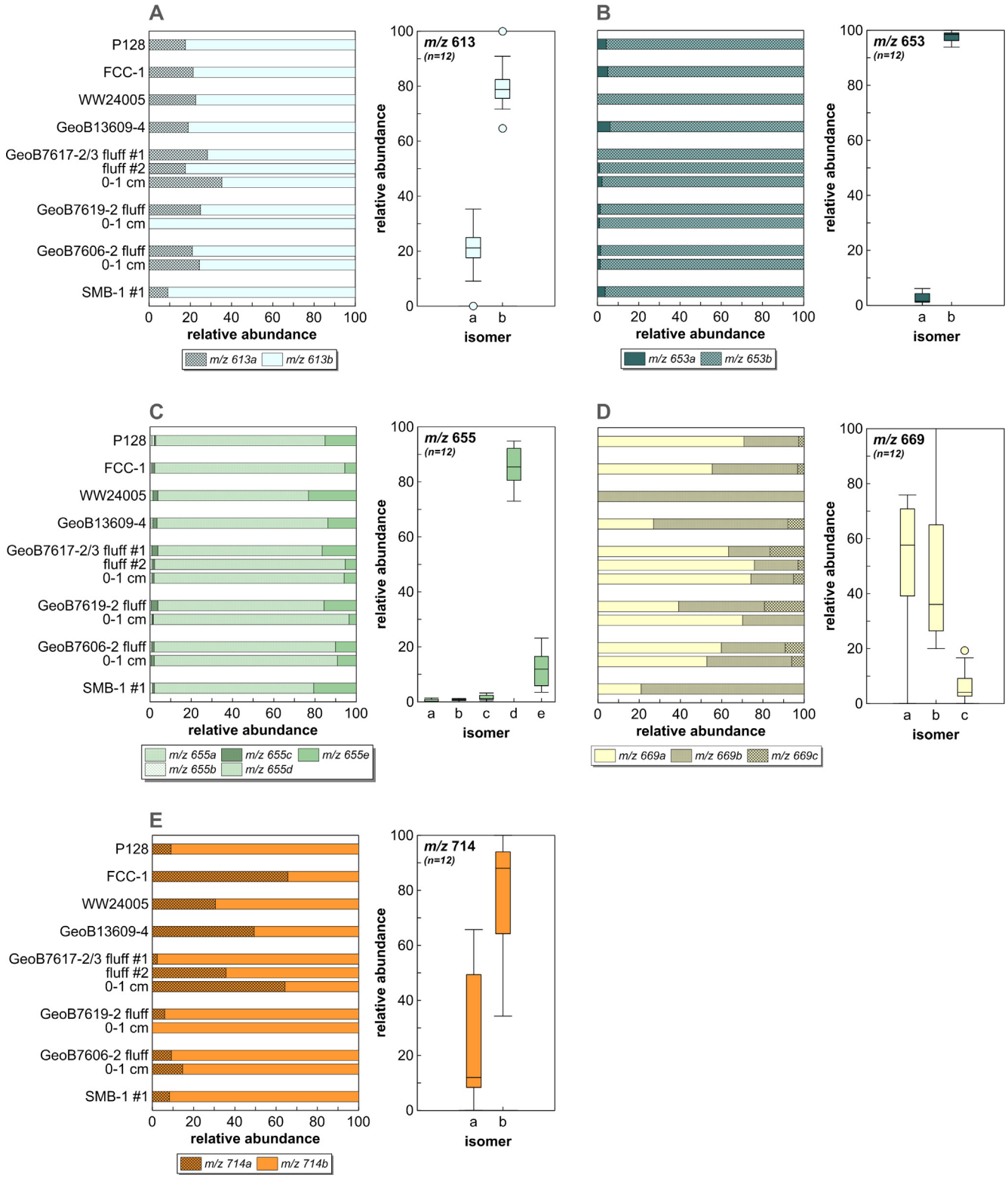

Fig. 5. Relative abundances of structural isomers for each BHP population of the investigated core-top sediments. Corresponding box-whisker plots are shown in Tukey style with IQR factors of 1.5.

contribution from its minor isomer *m/z* 613a (Fig. 5A), which accounts for 9–35% and of the anhydroBHT inventory. In contrast to these compounds, the relative isomer abundances of Me-BHT (Fig. 5D) and aminotriol (Fig. 5E) are much more heterogeneous between samples and some of the observed heterogeneity appears to be linked to environmental conditions or sedimentary setting (Fig. 5, Table 1). The concentrations of some isomers including *m/z* 655a and all Me-BHT isomers (Table 2) are significantly higher in the river-dominated settings from the Black Sea (P128) and the Gulf of Mexico (FCC-1). The accumulation of these compounds is likely indicative of the contribution of terrigenous BHPs (Pearson et al., 2009) indicating that they could be useful in tracing terrestrial organic matter input. However, all sediment samples from oxic water columns (P128, FCC-1, and *GeoB*13609-4) are also characterized by overall higher abundances of anhydro-BHT (summed isomers; Table 2; Fig. 6), consistent with the use of anhydro-BHT as degradation proxy. Likewise, with the exception of two fluffy layer samples (the fresh suspended matter at the sediment-water interface) from the deep Black Sea (*GeoB*7619-2 and *GeoB*7606-2), *m/z* 655a only occurs in the oxic core-top samples and was not detected in any of the anoxic sediments (Fig. 5C). Also, the aminotriol populations overall are characterized by higher abundances of the *m/z* 714a isomer (9–66%) in oxic and oxygen-limited (upwelling-influenced) settings, while the anoxic sediments appear to contain predominantly *m/z* 714b (36–100%; Fig. 5E). Some isomer abundances also seem to be altered under the anoxic conditions of the Black Sea (samples *GeoB*7606-2, *GeoB*7617-2/3 and *GeoB*7619-2). The relative abundance of *m/z* 653a and *m/z* 655c (Table 2 and Fig. 5B and C) increases from the fluffy layer into the sedimentary core-top while *m/z* 655e shows the opposite trend. This pattern might be caused by preferential degradation but could alternatively indicate contributions from different bacterial communities present in the water column and sediment.

BHT isomer *m/z* 655e (BHT II), proposed as proxy for water column suboxia, anoxia, and/or anammox (Sáenz et al., 2011b; Rush et al., 2014), is present in all samples irrespective of redox conditions. Thus, its presence alone cannot be used as an exclusive proxy for suboxia/anoxia or anammox. Instead, the BHT II ratio (*m/z* 655e over the sum of *m/z* 655d and *m/z* 655e; Rush et al., 2014, Matys et al., 2017) seems to be a better indicator for redox conditions. BHT II ratios in the river-dominated samples P128 (0.16) and FCC-1 (0.06) are as high as BHT II ratios in the anoxic Black Sea samples (0.05–0.17), which may indicate that a substantial amount of *m/z* 655e also derives from the continent. However, the highest BHT II ratio (0.24) is found in sample WW24005, which is influenced by an upwelling-induced oxygen minimum zone, and BHT II ratios in the Chilean oxygen minimum zone and a marine anammox enrichment culture ("*Candidatus* Scalindua profunda") are well above 0.50 (Rush et al., 2014; Matys et al., 2017). Accordingly, the BHT II ratio may serve as a proxy for anoxia/anammox above a certain threshold value, but additional data – including compound-specific $\delta^{13}C$ data (Hemingway et al., 2018) – from various environments are required to determine this threshold value.

Our current data set is too small to convincingly determine whether certain isomers are in fact indicative of environmental settings or redox conditions. However, the observed isomer distributions present intriguing potential for new environmental proxies and highlight the potential to further evaluate the influence of environmental conditions on BHP isomer diversity. The accumulation of isomers such as *m/z* 655a and *m/z* 714a under oxic conditions holds potential to use them as proxies for redox conditions and the changing abundances of 653a and *m/z* 655c vs *m/z* 655e between fluffy layer and core-top sediment samples in the Black Sea may indicate their usefulness in tracing degradation or, alternatively, bacterial communities. Certainly, additional data from sediments retrieved from a range of environmental conditions

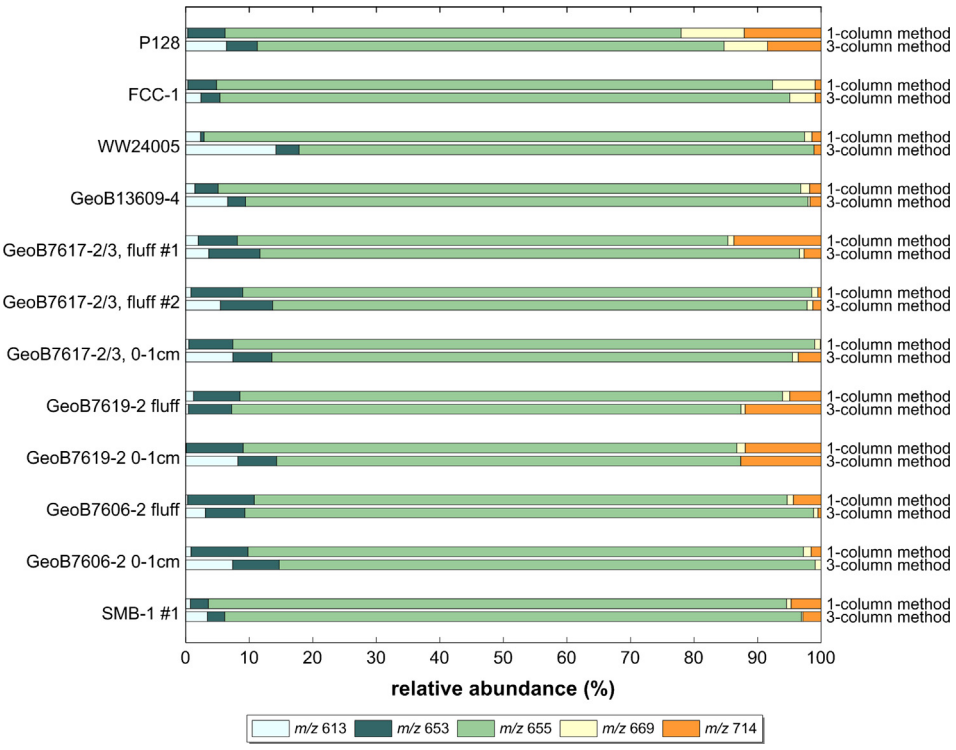

Fig. 6. Comparison of BHP relative abundances (MS response) determined using the 1-column method of Talbot et al. (2003a) and the 3-column method described here. BHP relative abundances represent the summed relative abundance of all isomers detected for each BHP using the respective method.

are required to confirm the proxy potential of several of the new BHP isomers and such isomer abundance data would ideally be aided by metagenomic data.

3.3. Effect on BHP quantification

Fig. 6 shows the relative abundances of summed BHP isomers detected using the 3-column method in comparison to the established 1-column method of Talbot et al. (2003a). The relative distributions in the investigated samples differ between methods implying that robust BHP quantification relies on good chromatographic separation of structural isomers within each BHP population. This is particularly obvious for anhydro-BHT, unsat. anhydro-BHT, and aminotriol. As stated above (Section 2.2), analyses were performed on splits of each acetylated sedimentary TLE, i.e., differences observed between chromatographic methods cannot derive from different acetylation yields (or other wet-chemical processing). Thus, these differences likely stem from ion suppression effects caused by co-elution of different BHP isomers as well as co-elution with other compounds. With the lower chromatographic resolution (*Rs*) of the standard method, many BHPs are not baseline-resolved or co-elute. For example, *Rs* calculated at half peak height (Snyder et al., 1997) is 0.39 for the *m/z* 714b and *m/z* 653b peaks and 0.54 for the *m/z* 669a and *m/z* 655e peaks (Table 3). Likewise, isomer pairs such as *m/z* 655d and *m/z* 655e (*Rs* = 1.56) or *m/z* 669a and *m/z* 669b (*Rs* = 2.42) do not show full baseline separation. Hence, isomers of a specific BHP may either: (i) not be separated chromatographically and thus enter the MS as a more efficiently ionized pooled fraction, resulting in high response; or conversely, (ii) may co-elute with other BHPs and become suppressed due to low ion abundance or other ion interferences. The chromatographic resolution could be significantly improved with the 3-column method and many isomer pairs are fully baseline-resolved including abovementioned *m/z* 655d and *m/z* 655e (*Rs* = 3.49) or *m/z* 669a and *m/z* 669b (*Rs* = 4.42). The resolution between each of the critical new isomer pairs is >2 (Table 3) except for the BHT *m/z* 655a and *m/z* 655b peaks (*Rs* = 0.85) and *m/z* 655b and *m/z* 655c peaks (*Rs* = 1.52), which results from their low concentrations (i.e., high peak width to peak height ratio). Nonetheless, while all of the smaller BHP isomers are detectable using the 3-column UHPLC/QQQ method, many still are not baseline-separated from other BHPs. For example, aminotriol isomer *m/z* 714a co-elutes with unsat. BHT isomers *m/z* 653b (*Rs* = 0.08) and *m/z* 653b (*Rs* = 0.68) (Table 3, Fig. 3). Accordingly, ion suppression effects will impact BHP quantification, even with the 3-column method, although to a lesser degree due to the generally improved resolution. In order to truly assess the effect of ion suppression on BHP quantification between the 1-column and 3-column methods, authentic standards would be required, which unfortunately are not available.

Table 3
Chromatographic resolution (*Rs*) calculated at half peak height of critical BHP pairs (according to retention time) between the 1-column and 3-column method and for critical new BHP isomer pairs detected with the 3-column method.

Critical pair	1-column method	3-column method
m/z 714b, *m/z* 653b	0.39	0.68
m/z 655d, *m/z* 669a	2.06	2.45
m/z 669a, *m/z* 655e	0.54	0.31
m/z 655d, *m/z* 655e	1.56	3.45
m/z 669a, *m/z* 669b	2.42	4.42
m/z 714a, *m/z* 653a		0.08
m/z 714a, *m/z* 714b		2.20
m/z 653a, *m/z* 653b		2.54
m/z 714a, *m/z* 653b		2.83
m/z 653b, *m/z* 655a		1.65
m/z 655a, *m/z* 655b		0.85
m/z 655b, *m/z* 655c		1.52
m/z 655c, *m/z* 655d		4.38
m/z 669a, *m/z* 669c		3.16
m/z 669c, *m/z* 613a		1.61

4. Conclusions

The new 3-column method developed here reveals several new BHP isomers in marine sedimentary core-top samples. The relative abundance of BHP isomers changes significantly between the investigated samples and the abundance of some isomers seem to be linked to specific environmental conditions. Improved chromatographic separation of structural BHP isomers will enhance quantification of absolute and relative BHP abundances, paves the way for environmental proxy development, and holds promise that these improved separation methods will be useful for future compound-specific isotope work (Hemingway et al., 2018).

Acknowledgements

This project was funded through Deutsche Forschungsgemeinschaft grant KU2842/1-1 to S.K., a National Science Foundation grant #EAR-1349126, NASA-NAI funding (CAN-6; MIT team), and the Gordon and Betty Moore Foundation (to A.P.). We thank Stuart Wakeham, Gesine Mollenhauer and Elizabeth A. Canuel who generously provided sample material, and Paula V. Welander who provided the lipid extract of the *R. palustris* TIE-1 culture. We also thank Associate Editor Bart van Dongen and two anonymous reviewers for helpful comments that improved this manuscript.

Associate Editor—**Bart van Dongen**

References

Bisseret, P., Rohmer, M., 1989. Bacterial sterol surrogates. Determination of the absolute configuration of bacteriohopanetetrol side chain by hemisynthesis of its diastereoisomers. The Journal of Organic Chemistry 54, 2958–2964.

Blumenberg, M., Mollenhauer, G., Zabel, M., Reimer, A., Thiel, V., 2010. Decoupling of bio- and geohopanoids in sediments of the Benguela Upwelling System (BUS). Organic Geochemistry 41, 1119–1129.

Cooke, M.P., Talbot, H.M., Wagner, T., 2008. Tracking soil organic carbon transport to continental margin sediments using soil-specific hopanoid biomarkers: a case study from the Congo fan (ODP site 1075). Organic Geochemistry 39, 965–971.

Coolen, M.J.L., Talbot, H.M., Abbas, B.A., Ward, C., Schouten, S., Volkman, J.K., Sinninghe Damsté, J.S., 2008. Sources for sedimentary bacteriohopanepolyols as revealed by 16S rDNA stratigraphy. Environmental Microbiology 10, 1783–1803.

Eickhoff, M., Birgel, D., Talbot, H.M., Peckmann, J., Kappler, A., 2014. Diagenetic degradation products of bacteriohopanepolyols produced by *Rhodopseudomonas palustris* strain TIE-1. Organic Geochemistry 68, 31–38.

Hemingway, J., Kusch, S., Shah Walter, S.R., Polik, C.A., Elling, F.J., Pearson, A., 2018. A novel method to measure the ^{13}C composition of intact bacteriohopanepolyols. Organic Geochemistry 123, 144–147.

Jorgensen, B.B., Arz, H., Böttcher, M.E., Dehning, K., Glaeser, J., Kaiser, E., Kahl, G., Kallmeyer, J., Klann, M., Klockgether, G., Kuypers, M., Lamy, F., Lavik, G., Leipe, T., Neretin, L., Naumann, K., Nilgrün, O., Pease, T., Pollehne, F., Schäfer, R., Scheurle, C., Schippers, A., Secieru, D., Seiter, C.D., Sliekers, O., Sterz, M., Theune, A., Truscheit, T., Wehausen, R., Wienberg, C., 2003. Meteor-Berichte 03-1, Ostatlantik-Mittelmeer-Schwarzes Meer Part 4, Cruise No. 51, Leg 4, Leitstelle Meteor, Institut für Meereskunde der Universität Hamburg.

Matys, E.D., Sepúlveda, J., Pantoja, S., Lange, C.B., Caniupán, M., Lamy, F., Summons, R.E., 2017. Bacteriohopanepolyols along redox gradients in the Humboldt Current System off northern Chile. Geobiology 15, 844–857.

Neunlist, S., Rohmer, M., 1988. A convenient route to an acetylenic C_{35} hopanoid and the absolute configuration of the side-chain of aminobacteriohopanetriol. Journal of the Chemical Society Chemical Communications, 830–832.

Ourisson, G., Albrecht, P., 1992. Hopanoids. 1. Geohopanoids: the most abundant natural products on Earth? Accounts of Chemical Research 25, 398–402.

Pearson, A., 2000. Biogeochemical Applications of Compound-Specific Radiocarbon Analysis. PhD thesis. MIT/WHOI Joint Program, USA.

Pearson, A., Rusch, D.B., 2008. Distribution of microbial terpenoid lipid cyclases in the global ocean metagenome. The ISME Journal 3, 352–363.

Pearson, A., Leavitt, W.D., Sáenz, J.P., Summons, R.E., Tam, M.C.M., Close, H.G., 2009. Diversity of hopanoids and squalene-hopene cyclases across a tropical land-sea gradient. Environmental Microbiology 11, 1208–1223.

Rosa-Putra, S., Nalin, R., Domenach, A.M., Rohmer, M., 2001. Novel hopanoids from *Frankia* spp. and related soil bacteria – Squalene cyclization and significance of geological biomarkers revisited. European Journal of Biochemistry 268, 4300–4306.

Rush, D., Sinninghe Damsté, J.S., Poulton, S.W., Thamdrup, B., Garside, A.L., González, J.A., Schouten, S., Jetten, M.S.M., Talbot, H.M., 2014. Anaerobic ammonium-oxidising bacteria: a biological source of the bacteriohopanetetrol stereoisomer in marine sediments. Geochimica et Cosmochimica Acta 140, 50–64.

Sáenz, J.P., Eglinton, T.I., Summons, R.E., 2011a. Abundance and structural diversity of bacteriohopanepolyols in suspended particulate matter along a river to ocean transect. Organic Geochemistry 42, 774–780.

Sáenz, J.P., Wakeham, S.G., Eglinton, T.I., Summons, R.E., 2011b. New constraints on the provenance of hopanoids in the marine geologic record: bacteriohopanepolyols in marine suboxic and anoxic environments. Organic Geochemistry 42, 1351–1362.

Schaeffer, P., Schmitt, G., Adam, P., Rohmer, M., 2008. Acid-catalyzed formation of 32,35-anhydrobacteriohopanetetrol from bacteriohopanetetrol. Organic Geochemistry 39, 1479–1482.

Snyder, L.R., Kirkland, J.J., Glajch, J.L., 1997. Practical HPLC Method Development. John Wiley and Sons, Hoboken, NJ, USA.

Stampf, P., Herrmann, D., Bisseret, P., Rohmer, M., 1991. 2α-Methylhopanoids: first recognition in the bacterium *Methylobacterium organophilum* and obtention via sulphur induced isomerization of 2β-methylhopanoids: an account for their presence in sediments. Tetrahedron 47, 7081–7090.

Talbot, H.M., Rohmer, M., Farrimond, P., 2007a. Rapid structural elucidation of composite bacterial hopanoids by atmospheric pressure chemical ionisation liquid chromatography/ion trap mass spectrometry. Rapid Communications in Mass Spectrometry 21, 880–892.

Talbot, H.M., Rohmer, M., Farrimond, P., 2007b. Structural characterisation of unsaturated bacterial hopanoids by atmospheric pressure chemical ionisation liquid chromatography/ion trap mass spectrometry. Rapid Communications in Mass Spectrometry 21, 1613–1622.

Talbot, H.M., Coolen, M.J.L., Sinninghe Damsté, J.S., 2008a. An unusual 17α,21β(H)-bacteriohopanetetrol in Holocene sediments from Ace Lake (Antarctica). Organic Geochemistry 39, 1029–1032.

Talbot, H.M., Squier, A.H., Keely, B.J., Farrimond, P., 2003a. Atmospheric pressure chemical ionisation reversed-phase liquid chromatography/ion trap mass spectrometry of intact bacteriohopanepolyols. Rapid Communications in Mass Spectrometry 17, 728–737.

Talbot, H.M., Watson, D.F., Pearson, E.J., Farrimond, P., 2003b. Diverse biohopanoid compositions of non-marine sediments. Organic Geochemistry 34, 1353–1371.

Talbot, H.M., Summons, R.E., Jahnke, L.L., Cockell, C.S., Rohmer, M., Farrimond, P., 2008b. Cyanobacterial bacteriohopanepolyol signatures from cultures and natural environmental settings. Organic Geochemistry 39, 232–263.

Talbot, H.M., Bischoff, J., Inglis, G.N., Collinson, M.E., Pancost, R.D., 2016. Polyfunctionalised bio- and geohopanoids in the Eocene Cobham Lignite. Organic Geochemistry 96, 77–92.

van Dongen, B.E., Talbot, H.M., Schouten, S., Pearson, P.N., Pancost, R.D., 2006. Well preserved Palaeogene and Cretaceous biomarkers from the Kilwa area, Tanzania. Organic Geochemistry 37, 539–557.

van Winden, J.F., Talbot, H.M., Kip, N., Reichart, G.-J., Pol, A., McNamara, N.P., Jetten, M.S.M., Op den Camp, H.J.M., Sinninghe Damsté, J.S., 2012. Bacteriohopanepolyol signatures as markers for methanotrophic bacteria in peat moss. Geochimica et Cosmochimica Acta 77, 52–61.

Wu, C.H., Kong, L., Bialecka-Fornal, M., Park, S., Thompson, A.L., Kulkarni, G., Conway, S.J., Newman, D.K., 2015. Quantitative hopanoid analysis enables robust pattern detection and comparison between laboratories. Geobiology 13, 391–407.

Zhao, N., Berova, N., Nakanishi, K., Rohmer, M., 1996. Structures of two bacteriohopanoids with acyclic pentol side-chains from the cyanobacterium *Nostoc* PCC 6720. Tetrahedron 52, 2777–2788.

Zhu, C., Talbot, H.M., Wagner, T., Pan, J.-M., Pancost, R.D., 2011. Distribution of hopanoids along a land to sea transect: implications for microbial ecology and the use of hopanoids in environmental studies. Limnology and Oceanography 56, 1850–1865.

Zundel, M., Rohmer, M., 1985. Prokaryotic triterpenoids. 1. 3β-Methylhopanoids from *Acetobacter* species and *Methylococcus capsulatus*. European Journal of Biochemistry 150, 23–27.